An effective grain growth model using a combination of Voronoi tessellation and Monte Carlo method.

Chihak Ahn
TCAD lab
Samsung Semiconductor Inc.
San Jose, CA, United States
chihak.ahn@samsung.com

Seonghoon Jin
TCAD lab
Samsung Semiconductor Inc.
San Jose, CA, United States
s.jin@samsung.com

Gijae Kang
*CSE team**
Samsung Electronics
Hwaseong-si, Korea
gijae.kang@samsung.com

Joohyun Jeon
CSE team
Samsung Electronics
Hwaseong-si, Korea
jooh.jeon@samsung.com

Hyoshin Ahn
CSE team
Samsung Electronics
Hwaseong-si, Korea
hyoshin.ahn@samsung.com

Inkook Jang
CSE team
Samsung Electronics
Hwaseong-si, Korea
inkook.jang@samsung.com

Woosung Choi
TCAD lab
Samsung Semiconductor Inc.
San Jose, CA, United States
woosung.c@samsung.com

Dae Sin Kim
CSE team
Samsung Electronics
Hwaseong-si, Korea
daesin.kim@samsung.com

* Computational Science & Engineering team

***Abstract*—We present an efficient simulation method for metal grain growth that combines Voronoi tessellation and the Monte Carlo method. The accuracy of our model is validated through its ability to reproduce theoretical predictions of film stress and grain boundary energy. The model can identify stress hot spots and generate grain size statistics potentially useful for estimating metal line failure. Our results demonstrate the utility of this approach for studying metal grain growth and its impact on device failure.**

***Index Terms*—DRAM metal line, grain growth, film stress, voids formation**

I. Introduction

In state-of-the-art semiconductor fabrication, controlling the grain growth in the metal lines is important to prevent device failure. From a macroscopic point of view, grains grow as long as the total free energy of the system decreases while the three major energies (the stress energy, the grain boundary energy, and the surface energy) compete with each other [1]. At the microscopic level, multiple physics processes are involved, including diffusion, nano-void formation, slipping, and dislocation formation, making it challenging to develop a comprehensive simulation model. Various methods have been developed to tackle this challenge, such as molecular dynamics [2], the phase field method [3], Monte Carlo method [4], and combinations of these methods [4]. A brief summary of these methodologies can be found in Ref. [2].

To tackle this intricate issue, we have developed a simple yet effective model utilizing Voronoi tessellation [5] and the Monte Carlo method. The underlying concept of our approach is that the atom density at grain boundaries differs from the density inside the grain [1], [6]. Additionally, we enforce the conservation of the total number of atoms during grain growth. Based on these principles, we study two distinct types of evolution models: the void evolution model and the stress evolution model (Fig. 1). These models represent two limiting cases that can be modeled relatively easily.

The first limiting case, void formation, conserves the total grain boundary volume without any stress buildup. In this case, the total grain volume and the total grain boundary volume are conserved separately. As a result, the grain boundary thickens as grains grow, which can be accounted for as nano-voids. In the second case, where stress builds up, a constant thickness of the grain boundary layer is assumed. As the total grain boundary area decreases to reduce the grain boundary energy during grain growth, the total grain boundary volume also decreases. To compensate for the decreasing grain boundary volume, grains must stretch to occupy the space with the same number of atoms, resulting in the generation of tensile stress. However, since the entire reduced grain boundary volume is converted to the tensile strain in this model, it excludes the possibility of slipping among grains, making it a limiting case. In reality, the situation lies between the two limiting cases, where partial stress relaxation with nano-void formation happens simultaneously.

II. Methods

A. Granular region generation and grain growth model

Initially, if a non-zero initial stress is expected, stress is calculated based on the deposition conditions. Then the grain seeds are randomly distributed to achieve the desired average initial seed density in a fine mesh that can resolve the grain boundaries. The entire simulation domain undergoes Voronoi tessellation to generate the initial grain distribution. If the initial size distribution or the grain boundary thickness is

position dependent, it is important to appropriately reflect these initial conditions in the seed distribution or thickness, as the final result is strongly influenced by the initial conditions. At each mesh node, the initial grain field (A) is defined with a function of the distance (l) to the bisecting plane of the two nearest seeds:

$$A = 1 - f(l), \tag{1}$$

where $f(l)$ is a function of the distance that ranges from 0 to 1. In all the examples presented here, we used $f(l) = \exp(-l^2/l_c^2)$ where l_c is the characteristic length. When the value of A is lower than the pre-defined threshold value, the mesh node is considered as a boundary node. The threshold value and l_c were defined to make the initial grain boundary thickness to be 0.2 nm for comparison with Ref. [6]. In the void formation option, l_c is automatically adjusted to keep the local V_{GB} constant before and after each local tessellation. Conversely, in the strain buildup case, l_c remains constant throughout the simulation(Fig. 1).

Grain growth simulation begins by selecting a grain to be cannibalized by its neighbors. The seed of the selected grain is removed, and the surrounding region of the grain undergoes local tessellation. The purpose of the local tessellation is to confine the local effects within the tessellation area during the void formation or the strain evolution. To facilitate efficient local tessellation, all mesh nodes within a grain are grouped based on the nearest neighbor grain index. Fig. 2 shows the example of the local tessellation. In Fig. 2a), the grain at the center is selected for removal. The area enclosed by the white broken lines in Fig. 2c) represents the minimal local tessellation area. With a larger tessellation area, the results are averaged within that area. In the case of the void formation model, the newly generated boundary is considered as a void. The selection of the grain is performed using the Monte Carlo method. This process continues until the average grain size reaches the specified final grain size.

Grain selection rate is modeled with the effective activation energy composed of the size-, stress-, and interface-dependent activation energy, and given by:

$$r = r_0 \exp\left(-\frac{E_a}{kT}\right), \tag{2}$$

$$E_a = k_{\text{size}} \left(\frac{s}{s_0}\right)^p + k_{\text{stress}} u + \Delta E_b, \tag{3}$$

where r_0 is the effective rate constant, k the Boltzmann constant, T the absolute temperature, E_a the effective activation energy, k_{size} the energy constant of the grain size dependence, s the grain size, s_0 the reference grain size, p the power factor, k_{stress} the stress energy constant, u the stress energy density, and ΔE_b the energy change from any additional effect such as a boundary effect. The size of each grain (s) is calculated using the square or cube approximation method.

In Eq. 3, the first term is designed to capture the phenomenon of Ostwald ripening or grain coarsening [7], with a positive k_{size}. This term accounts for the merging of smaller grains into larger ones over time. The second term represents the influence of the stress on the growth rate, and the last term includes all other free energies associated with the grain merging. One example of the third term is the binding energy at material interfaces, which can change the merging rate.

Although the rate expression bears some resemblance to the rate of the kinetic Monte Carlo method, it is important to note that it is an effective parameter and does not directly correspond to a specific microscopic physical process. This

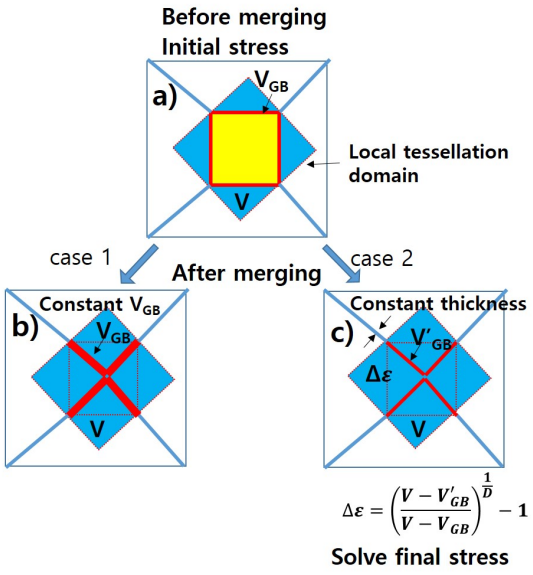

Fig. 1. Two limiting cases of the grain growth model. a) Local tessellation domain, b) void formation case, c) strain evolution case.

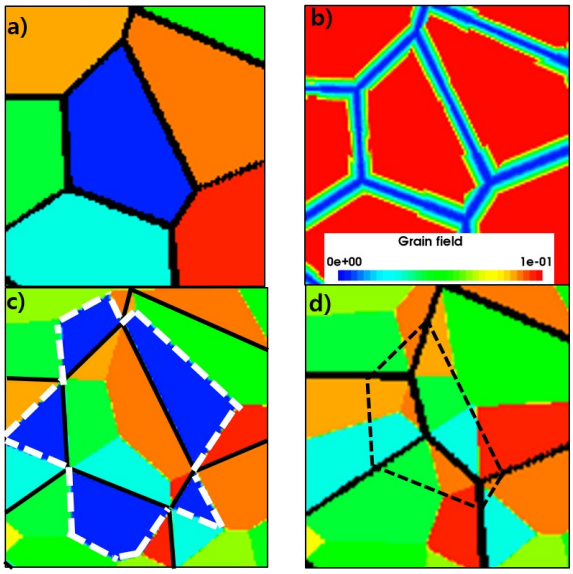

Fig. 2. Grain growth example. a) grain index field with boundaries before removal, b) grain field, c) the minimal local tessellation area with neighbor grain index field, d) new grain boundaries with new neighbor index field after merging. The region in this example is the part of Fig. 5d) enclosed by the black line.

is because in the simulation, during a single grain removal and merging step, many atoms are simultaneously moving from one grain to its neighboring grains. As a result, the rate expression serves as an effective parameter that captures the overall behavior of grain merging in the simulation, rather than representing a specific microscopic process in detail.

While it is possible to solve the physical processes described by Eqs. 2 and 3 in a fully stress-coupled manner with a small structure, it is not practical for the applications of our interest due to computational burden associated with frequent stress simulation using a fine mesh. Therefore, in this report, we have employed a one-way stress coupling approach in which stress is not updated at each grain merging step and solved before and after the entire grain growth.

B. Void formation without stress buildup

The first limiting case (Fig. 1b) corresponds to grain growth without transient stress buildup, where the conservation of the total grain boundary volume (grain boundary area $\times$ thickness of the grain boundary) is required. To preserve the grain boundary volume, the thickness of the grain boundary should increase during grain growth, as the total grain boundary area tends to decrease. In Fig. 1b), the thick red region represents the newly created void volume resulting from a grain merging step. In a real situation, the shape of the void changes to reduce the surface area through a diffusion process. However, in our model, our primary focus is on the volume of the void, and the generation of a realistic void shape is not pursued.

C. Stress buildup without void formation

The other limiting case (Fig. 1c) is the stress buildup without a void formation. The analytic strain is given by

$$\varepsilon = \frac{\frac{a}{d_0} - \frac{a}{d}}{1 - \frac{a}{d_0}} \approx \left(\frac{a}{d_0} - \frac{a}{d}\right)\left(1 + \frac{a}{d_0}\right), \tag{4}$$

where d_0 is the initial grain size, d the final grain size, and a the grain boundary thickness (Fig. 3). Although Eq. 4 is derived with a two-dimensional structure, it is also true for the three dimension.

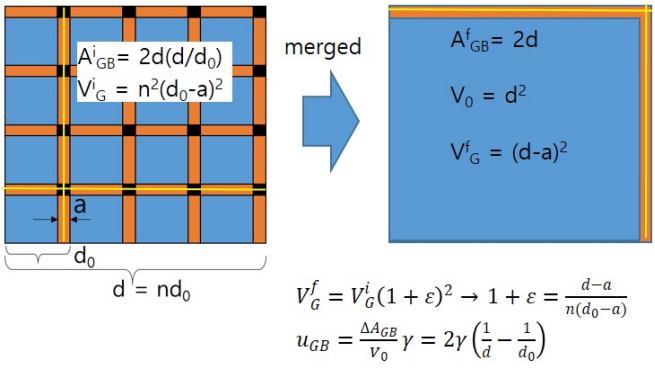

Fig. 3. Two dimensional grain merging schematic to derive the strain and the grain boundary energy.

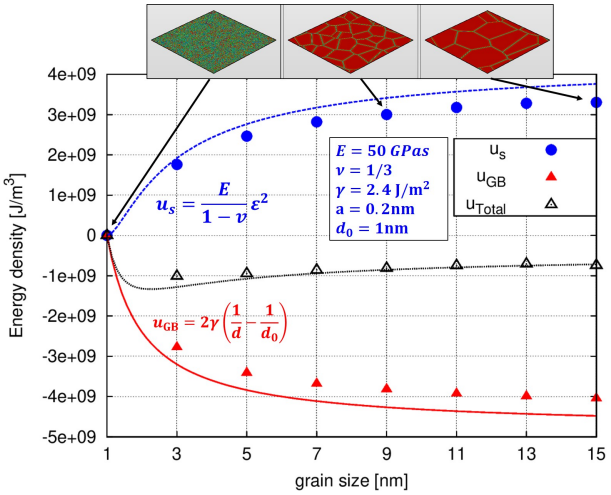

Fig. 4. Comparison of energies between simulations (symbols) and the analytic model (lines) for two-dimensional grain growth.

Eq. 4 is similar to the strain in Ref [6] with an extra factor 2 and more rigorous extension. We got the same analytic grain boundary energy as Ref [6] which is given by

$$u_{GB} = \beta\gamma\left(\frac{1}{d} - \frac{1}{d_0}\right), \tag{5}$$

where β is the dimension of the growth space, and γ the grain boundary energy density.

In grain growth simulation, the change of strain is calculated locally at each grain merging step and it is given by

$$\Delta\varepsilon = \left(\frac{V - V'_{GB}}{V - V_{GB}}\right)^{\frac{1}{D}} - 1, \tag{6}$$

where V is the local tessellation volume, V'_{GB} the newly generated grain boundary volume after local tessellation using the constant grain boundary thickness, V_{GB} the grain boundary volume before grain merging, and D the growth dimension.

III. Results and Discussion

Because our model, particularly Eq. 3, is not derived rigorously from a fundamental physics equation, it is essential to carefully check the validity by comparing the results with experimental observations or other theoretical studies. As an initial step, we applied our model to a simple two-dimensional grain growth scenario, as depicted in Fig. 4. The comparison between the analytic model using Eqs. 4-5 and the numerical simulations employing Eqs. 2, 3, and 6 demonstrates a good agreement. In this simple structure, the initial conditions (d_0 and a in Eq. 4 of analytic model, and the intial grain size and the l_c in the simulation model) play a critical role in determining the strain and the void size during the grain growth. Additionally, we studied the grain size distribution by conducting 300 sample runs with a simple 50$\times$50 nm^2 planar structure. The obtained size distribution closely aligns with a log-normal distribution (Fig. 6), consistent with findings from many previous studies [3], [8], [9].

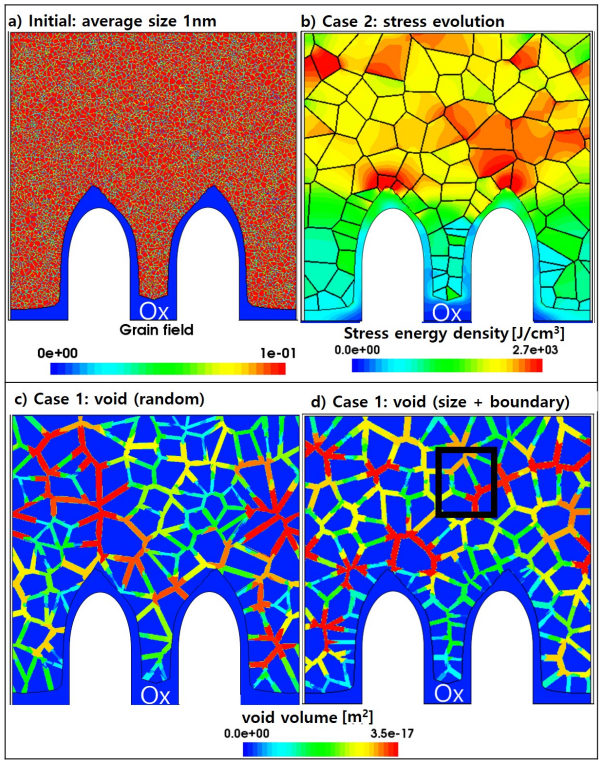

Fig. 5. Two limiting cases of grain growth. a) the initial distribution with the average size of 1nm. b) the stress energy density with the strain buildup scenario. c) the void formation scenario with random grain selection. d) the void formation scenario with size dependent selection plus the boundary effects. For b) and d), $T = 700K$, k_{size} =1eV, k_{stress} =0, s_0 =10nm, p =0.33, and ΔE_b =0.2eV were used. In case c), k_{size} =0 and ΔE_b =0. For stress simulation, E=100 GPa and ν=0.28.

As the next step, we applied the model to a simplified two-dimensional toy structure of the DRAM metal line. The results of the two scenarios are shown in Fig. 5. In case b) and d), we incorporated boundary effects by assigning $\Delta E_b = 0.2$ eV to the grains at the oxide boundary. The stress evolution model reveals a stress concentration near the top of the corrugated oxide, which has the potential to cause an open circuit failure. Additionally, the presence of a positive ΔE_b leads to slower growth at the material boundary compared to the bulk, resulting in a visible seam at the center of the narrow trench, as shown in Fig. 7. These findings are consistent with the experimental transmission electron microscope (TEM) images (Figs. 14 and 22 in Ref. [10]).

IV. Conclusion

We have presented an efficient grain growth model that combines Voronoi tessellation and the Monte Carlo method. This model has demonstrated the capability to reproduce the stress energy and grain boundary energy predicted by a theory, as well as the typical log-normal grain size distribution observed in simple two-dimensional structures. By incorporating a simple conservation law to preserve the total number of atoms and considering boundary effects, our model

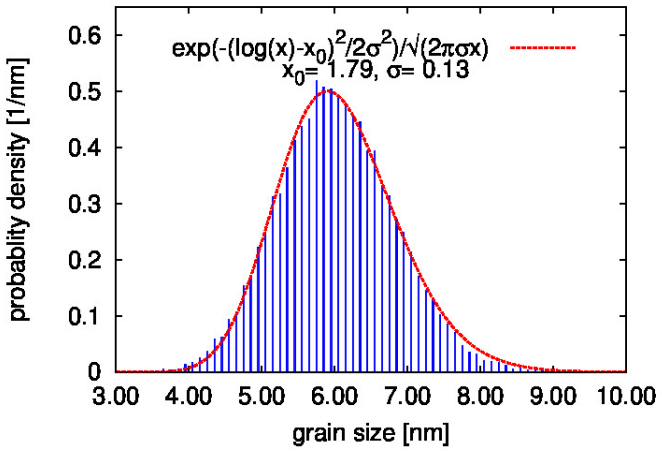

Fig. 6. Grain size ditribution after grain growth from 1nm initial average size to 6nm average size. Simulation was performed using a 50×50 nm^2 planar square with a periodic boundary condition. The line is the log-normal fit.

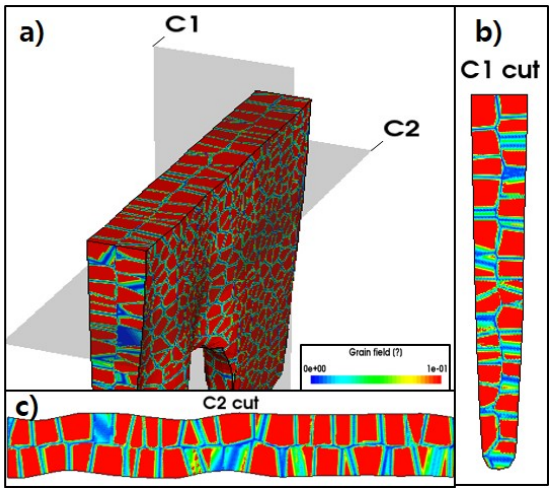

Fig. 7. Grain growth simulation in a DRAM metal line structure: a) three-dimensional view, b) vertical cross-section, c) horizontal cross-section. Simulation conditions are same as Fig. 5 d).

successfully reproduced the observed seam in a DRAM metal line and predicted the stress concentration hot spots.

References

[1] C.V. Thompson and R. Carel, J. Mech. Phys. Solids, **44**, No. 5, p657, 1996.
[2] E. Miyoshi, T. Takakib, Y. Shibuta, and M. Ohno, Comp. Mat. Sci. **152** p118, 2018.
[3] B. Korbuly *et. al.* Phys. Rev. E **95**, 053303, 2017.
[4] Y. Suwa, and Y. Saito, Mater. Trans. **46**, p1214, 2005.
[5] F. Aurenhammer, ACM Computing Surveys, **23**, No. 3, p345, 1991.
[6] P. Chaudhari, J. Vac. Sci & Tech B, **9**, p520, 1972.
[7] L. Latke and P.W. Voorhees, Growth and coarsening: Ostwald ripening in material processing, Springer-Verlag, Berlin, 2002.
[8] M. Fátima Vaz and M.A. Fortes, Scripta Metallurgica **22**, Issue 1, p35, 1988.
[9] H. J. Frost, C. V. Thompson, and D.T. Walton, Acta metall, mater. **38**, No. 8, p1455, 1990
[10] D. James, Advanced Semiconductor Manufacturing Conference (ASMC2013), p386, 2013.